

Dynamic and Residual Pore Water Pressure Response of Hybrid Foundation System Under Combined Action of Wind, Wave and Seismic Loading

Jiang Yang^{1,2,3}, Dingfeng Zhao⁴, Tao Fan^{1,2,3*}, Tian Sun^{5,6}

¹ Hubei Key Laboratory of Earthquake Early Warning, Hubei Earthquake Agency, Wuhan 430071, China

² Wuhan Institute of Seismic Instruments Co., Ltd., Xianning 437100, China

³ Engineering Technology Research Center for Earthquake Monitoring and Early Warning Disposal of Major Projects in Hubei Province, Xianning 437100, China

⁴ Shanghai Waterway Engineering Design and Consulting Co., Ltd., Shanghai 200120, China

⁵ College of Transportation Engineering, Nanjing Tech University, Nanjing, Jiangsu 210009, China

⁶ Jiangsu Sunpower Technology Co., Ltd., Nanjing 210009, China

* Corresponding author, e-mail: fant_cea@eqhb.gov.cn

Received: 14 August 2022, Accepted: 19 October 2022, Published online: 11 November 2022

Abstract

The dynamic response characteristics of the innovative marine wind power hybrid foundation under combined action of wind, wave and seismic loading are studied in this article. Taking the monopile foundation as reference group, the shearing strain-volumetric strain coupled pore pressure incremental constitutive model was utilized to simulate the kinetic behavior of seabed's saturated soil. The pressure distribution and variation characteristics of residual pore water pressure around pile foundation due to the interactions of upper structure, foundation and saturated soil are illustrated. The results indicate that: (a) the cylindrical platform changes the residual pore water pressure and accelerates the pressure accumulation area, which converts from surrounding the monopile to nearby the cylindrical platform; (b) compared to the hybrid foundation, the peak value of residual pore water accumulation of the monopile foundation is smaller only under seismic loading, which is due to that the monopile with smaller stiffness is more vulnerable to deform with soil synergistically; (c) the cylindrical platform structure can significantly reduce the horizontal placement extreme of pile foundation under the action of dynamic load, and can also change the distribution characteristics of bending moment of middle pile of the hybrid foundation. It is manifested by a lower bending moment extreme of the middle pile near the mudline under the action of wind and wave loading, while the seismic loading could increase the bending moment extreme of middle pile near the mudline.

Keywords

hybridpile foundation, pore water pressure, saturated soil, dynamic response, numerical simulation

1 Introduction

Because of the particularity of marine environment, the offshore wind turbines (OWTs) foundation suffers a long-term impact from such kinetic loading as wind wave, etc. In addition, most coastal regions are earthquake prone areas, making wind turbine foundation and tower to undertake the actions of wind wave and seismic loading simultaneously. Taking China's coastline as an example, although the development potential of offshore wind energy in the southeastern coastal region is huge, this region is an earthquake prone area, which requires a higher seismic capacity on offshore pile foundation due to geological activities. Therefore, it is necessary to optimize the design of the offshore wind turbine foundation and consider the multi-field

coupling effects on the anti-overturning capability of the offshore pile foundation [1, 2].

At present, the main foundation type includes monopile foundation, barrel foundation, multi-pile foundation, gravity foundation, jacket foundation, floating foundation, etc. [3, 4]. The monopile foundation is most popular due to its simple structure, easy to manufacture, and suitable for many working conditions, which accounts for 80% of the total existing offshore wind turbine foundation infrastructure [5]. Studies have shown that [6, 7], the anti-horizontal deformation and the anti-overturning capability of monopile foundation are usually important indicators for pile foundation design, and compared to the vertical loading

of tower's and wind turbines' dead load on pile foundation top, the wind wave action which may cause dynamic shear and dynamic bending moment on pile foundation is more destructive. The plastic limit analysis is considerable when determining the ultimate capacity of laterally loaded piles. Therefore, the influence of plastic deformation of soil and structures should be properly considered in the design of pile foundation [8–10]. Moreover, The circulatory load of wind and wave causes the pore water pressure of seabed surface soil to accumulate dynamically [11, 12], and when considering saturated soil-pile foundation interaction, due to the differences of the pile foundation surface and the seabed soil in water permeability and stiffness, the vibration of pile foundation under dynamic loading can cause the residual pore water pressure of soil around pile foundation to accelerate accumulating, which further causes significantly reduced soil carrying capacity and even soil liquefaction behavior [13–16]. The studies of Kourkoulis et al. [6] have shown that the dynamic loading caused by earthquake will not only greatly affect the vulnerability of monopile foundation and the upper wind turbine structure, but also will quicken the residual pore water pressure increase around the pile foundation. Besides, wind and wave loading also exerts a continuous effect on pile foundation, resulting in potential risks in offshore wind power foundation [17, 18].

For a deeper waters with strong seismic activity, it is uneconomical to eliminate the negative impact of the pore water pressure increase caused by environmental loading on its anti-overturning ability only by increasing the monopile length or the pile diameter, thus the concept of hybrid foundation is proposed and studied. Bienen et al. [19] studied the effect of adding wings around monopile on the pile foundation's anti-overturning ability through centrifuge experiments, and the results show that under the same horizontal loading, the existing of wings can significantly reduce pile deflection. Anastasopoulos and Theofilou [1] studied the anti-overturning ability of hybrid foundation combining monopile and platform under the effect of wind wave loading and seismic loading by numerical methods, and concluded that the vertical and horizontal bearing capacity of hybrid foundation is higher than monopile foundation, and that the influence of seismic loading on pile foundation's bearing capacity should be considered for regions with frequent seismic activities. Wang et al. [20–22] studied the deformation response of different cyclic loads, soil parameters and seismic to hybrid foundation by centrifuge experiments, used the vibration table to simulate the earthquake process, and investigated the liquefaction characteristics of

soil around pile foundation caused by residual pore water pressure. For the soil with poor drainage capacity, the reduction of soil shear modulus caused by residual pore water pressure should be considered [23]. Chen et al. [24] proposed a hybrid foundation which composed the monopile and wide-shallow bucket, and concluded that the cylindrical platform of this foundation can effectively share the horizontal loading and bending moment of monopile foundation, which is better than the monopile foundation in anti-overturning capacity.

The results of existing numerical simulation and model experiment also show that the residual pore water pressure around monopile foundation is one of the main factors leading to the decline of pile foundation's anti-overturning capacity [13], and the residual pore water pressure gradient changes obviously around pile foundation. In addition, saturated soil-pile foundation interaction (ISS) can not be negligible when simulating and analyzing the dynamic response of marine pile foundation [25, 26], meanwhile the seismic effect is also an important cause of residual pore water pressure accumulation [27]. However, the response characteristics of the new hybrid foundation under the coupling action of wind wave and seismic, especially when saturated soil-pile foundation interaction (ISS) is considered, the distribution characteristics of residual pore water pressure of the soil around the structure need to be studied.

The layout of this paper is prepared as follows: In Section 2 the Tower-Pile foundation-saturated soil interaction model was established using the ABAQUS finite element software, and the shear volumetric strain coupled pore water pressure incremental soil constitutive model was demonstrated. The load application method and the working conditions of numerical simulation are introduced in Section 3. The pile foundation-Saturated soil interaction model used to analyze the anti-horizontal deformation capability of pile foundations as well as the growth and distribution features of residual pore water pressure around two pile types under coupling loads in Section 4. The analysis results can provide theoretical basis for engineering design.

2 Numerical modeling

2.1 Hybrid foundation system

Compared to the traditional marine wind power monopile foundation, the new hybrid foundation has added a cylindrical platform structure around the monopile foundation, and its anti-overturning capacity under static loading has been widely verified [28]. But it is also critical to consider the dynamic interaction of tower, foundation and

saturated soil caused by wind, wave and seismic as well as the deduction of soil skeleton shear strength from the growth of residual pore water pressure in seabed's saturated soil due to dynamic loading.

In this study, the Vestas V90 3MW wind turbine was used, with the monopile diameter of 5 m, the length of pile below/above seabed as 30 m/10 m, and the monopile's steel pile thickness of 0.07 m. The height of upper tower structure is 90 m, the thickness of steel pipe piles of tower top and bottom is 0.05 m, the diameter of cylindrical platform is 15 m, and the marginal steel plate of platform extends into the seabed for 3 m. Between the cylindrical platform and the pile foundation, there is rib support to improve the anti-overturning capacity of the foundation. The thickness of the steel sheet used in platform is 0.03 m. The wind turbine's design and structural parameters are shown in Table 1.

The finite element models of the tower-foundation-soil of monopile and hybrid foundations are established separately by ABAQUS software. Due to the offshore pile foundation model is used to analyze the influences of environmental loads on offshore pile foundation foundations, it is more convenient to simplify part of the superstructure to concentrated mass and beam element rather than establish refined superstructure models. Therefore, the model has the following assumptions: (1) the superstructure is simplified as a concentrated mass; (2) The tower is simplified as a beam element; (3) Wind load and wave load are only applied to the structure by concentrated force. The above method can improve the calculation efficiency while reasonably considering the soil structure interaction.

In order to ensure numerical calculation accuracy and improve calculating efficiency, the soil mass is simulated with eight node linear reduced integral elements (C3D8R), the monopile foundation and cylindrical platform foundation are simulated with shell elements (S4R), the upper tower structure is simulated by beam elements (B31), and the wind turbine and such structures as blade are simulated with simplified lumped mass. At the same time, the Embed Interaction provided by ABAQUS interaction module

is used to embed the monopile foundation and cylindrical platform structure into soil mass to consider the soil-pile foundation interaction, while the binding function is applied to the contact surface of pile foundation and cylindrical platform. The tangent of cylindrical platform and soil surface is set with frictional contacts, the friction coefficient is set as 0.5, and the contact surface was set as hard contact [29]. The pile foundation top and the upper tower bottom were restrained by MPC beam to realize the transfer of axial force and bending moment from beam element to shell element. The schematic diagram of tower-foundation-soil finite element modeling is shown in Fig. 1.

2.2 Nonlinear dynamic constitutive behavior of soil

The upper structure and the foundation were simulated by elastic constitution. Rayleigh damping was selected as structural damping to simulate the energy dissipation process of metal material. But the nonlinear mechanical behavior of soil in dynamic load is relatively complicated [30]. Besides, the saturated soil as a two-phase medium, both the increased strain amplitude and accumulated residual pore water pressure can cause stiffness degradation of soil skeleton frame, further leading to the reduction or even complete loss of soil shear strength. Chen et al. [31], Ruan et al. [32] and Zhao et al. [33] based on the Davidenkov backbone curve, referred to the "extended Masing" rule and the "n times method" proposed by Pyke to establish a DCZ nonlinear constitutive stress-strain hysteresis curve, introduced the pore pressure increment model proposed by Martin et al. [34], and proposed

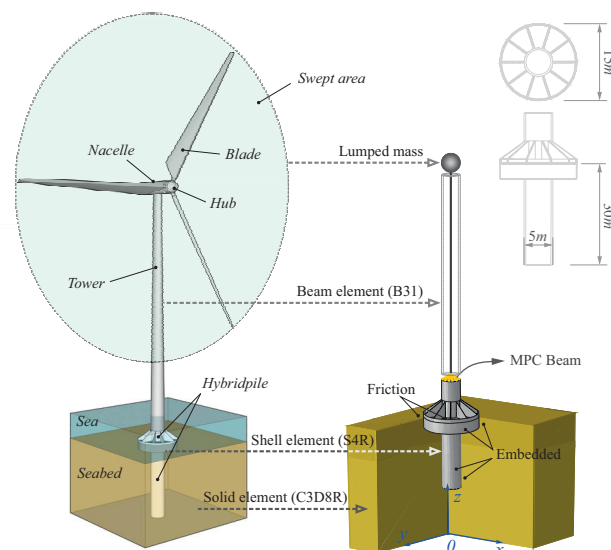


Fig. 1 Schematic diagram of tower-foundation-soil finite element modeling

Table 1 Wind turbine's design and structural parameters

Type of hub	Contrary wind, 3 blades
Height of tower structure	90 m
Weight of hub	41000 kg
Weight of nacelle	143000 kg
Weight of single blade	8400 kg
Length of single blade	44 m

a shear-volumetric strain coupled soil nonlinear pore water pressure increment model. The stress-strain loading-unloading hysteresis curve of modified Davidenkov constitutive model (total stress method) is shown in Fig. 2.

Based on the total stress method, Chen et al. [35] introduced the calculation formula of soil shear stiffness reduction by pore water pressure.

$$G_{\max}^t = G_{\max} \cdot (1 - u_e / \sigma'_{v0})^a, \quad (1)$$

where, G_{\max}^t is the shear modulus of hysteresis loop under strain reversal, G_{\max} is initial shear modulus, u_e is the residual pore water pressure, σ'_{v0} is the initial effective confining pressure, and a is intertwined with soil compaction. Wherein, the u_e is calculated by accumulating the pore pressure increment Δu_e of every loading/unloading cycle. Introducing the volume modulus E , the relationship between soil strain increment $\Delta \varepsilon_{vd}$ and pore water pressure increment Δu_e is as follows:

$$\Delta u_e = E \cdot \Delta \varepsilon_{vd}. \quad (2)$$

Byrne simplified the Martin et al. [34] model via the following novel incremental volumetric strain correlation:

$$\frac{\Delta \varepsilon_{vd}}{(\gamma_a - \gamma_{th})^{C_3}} = C_1 \exp\left(-C_2 \frac{\varepsilon_{vd}}{(\gamma_a - \gamma_{th})^{C_3}}\right) \quad (3)$$

The relationship between the volumetric strain ε_{vd} and the pore water pressure ratio r_u can be expressed as:

$$r_u = m \ln(n \varepsilon_{vd} + 1), \quad (4)$$

in which, the pore water pressure ratio r_u is calculated by the pore water pressure u_e and the initial effective confining pressure σ'_{v0} , and Δu_e and $\Delta \varepsilon_{vd}$ indicate the pore water pressure increment and volumetric strain increment caused by one loading-unloading cycle. Dobry, et al. [36] proposed the concept of threshold shear strain which was used to define the starting strain value of the residual pore water pressure accumulation. When the amplitude of shear strain γ_a is lower than the threshold shear strain γ_{th} , the residual pore water pressure will not be increased. For sandy soil, its γ_{th} is usually taken at 0.01% ~ 0.03%. C_1, C_2, C_3, m, n are the dimensionless constants associated with soil properties. The studies of Chen et al. [23] have shown that the product of constants C_2 and C_3 is a constant value 0.15. According to the Eq. (5), the volume modulus E can be calculated:

$$E = 100 \sigma'_{v0} m n \exp(-r_u / m). \quad (5)$$

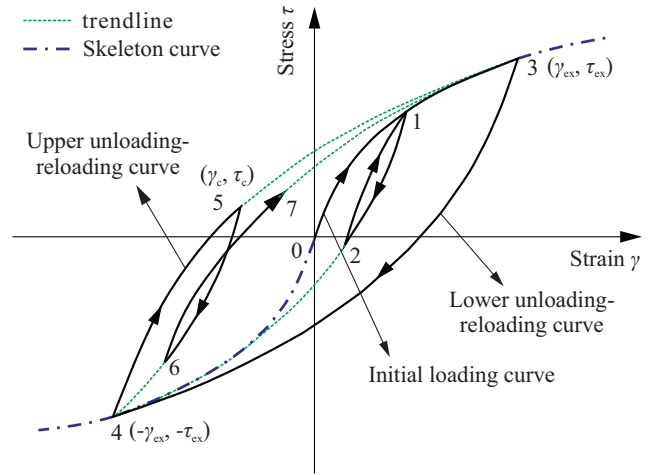


Fig. 2 Schematic diagram of nonlinear loading-unloading hysteresis curve

2.3 Numerical realization of soil constitutive model

The above-mentioned shear-volume strain coupled pore pressure increment model is based on the secondary development of ABAQUS/Explicit, and the ABAQUS software provides the constitutive model subroutine interface (VUMAT) under explicit dynamics analysis. Users can use Fortran language to compile the corresponding constitutive model according to requirements, and they only have to call the compiled script after finishing the compilation and submitting it for calculation. The subroutine implementation process is in Fig. 3.

This model is used to simulate the mechanical behavior of saturated soil surrounding marine pile foundation under environmental loads such as wind waves and earthquakes, and the soil under soil-structure interactions is divided into two layers for considering the change of soil strength with depth. The constitutive parameters of the superstructure and soil are shown in Table 2.

3 Environmental loading about simulation of OWTs

3.1 Load scheme selection

The structure of OWTs is often affected by environmental load, especially the structural resonance caused by dynamic loads may results in greater damage to the foundation and structure, so when designing the OWT structure, its natural frequency is usually designed outside the fan's running load frequency (between 1P and 3P) and the environmental load's dominant frequency. However, taking the monopile system of 3MW wind turbines as an example, its first-order natural frequency is typically between 0.24 Hz and 0.26 Hz [37], and the dominant frequency of wind load is low, so the high-frequency load can

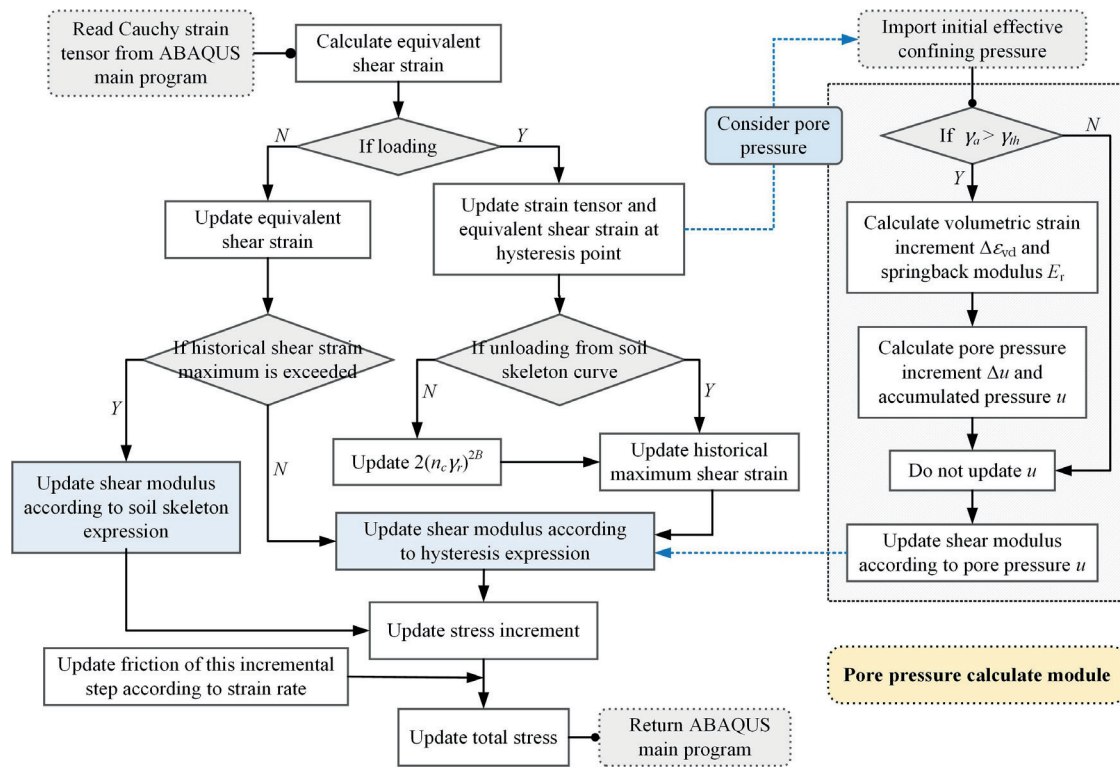


Fig. 3 Operation flow diagram of shear-volumetric strain coupled incremental pore pressure constitutive model

Table 2 Constitutive parameters of superstructure and soil

Material	G (MPa)	ν	A	$2B$	γ_r (%)	β	a	C_1	C_2	C_3	γ_{th} (%)	m	n
Steel	87500	0.2	—	—	—	—	—	—	—	—	—	—	—
Layer-1	24.52	0.49	1.03	0.74	0.065	0.003	0.5	0.921	0.163	1.25	0.005	0.345	668.9
Layer-2	96	0.48	1.1	0.88	0.09								

be ignored when considering the action of wind load on the system. The wind load is applied on the structure as a linearly enhanced load, and the dominant frequency of wave load may be close to the first-order natural frequency of the fan system, and the predominant frequency of the seismic load may also be close to high-order natural frequency of the fan system.

For a 3MW wind turbine system, the design value of wind load is set as 1 MN, the design amplitude of wave load is set as 2 NM. As for earthquake ground motion, the Kobe wave recorded in a magnitude-7.2 happened in Japan in 1995 is taken as the base rock input wave of the model for simulating strong earthquake action. In this wave band, the peak acceleration is 0.61 g, then the acceleration peak is adjusted to 0.2 g as the earthquake ground input. The seismic wave time-histories and the Fourier spectrum are shown in Fig. 4.

Selecting load application schemes is to compare the effect of environmental load on the loading capacity of monopile and hybrid foundations as well as the change in

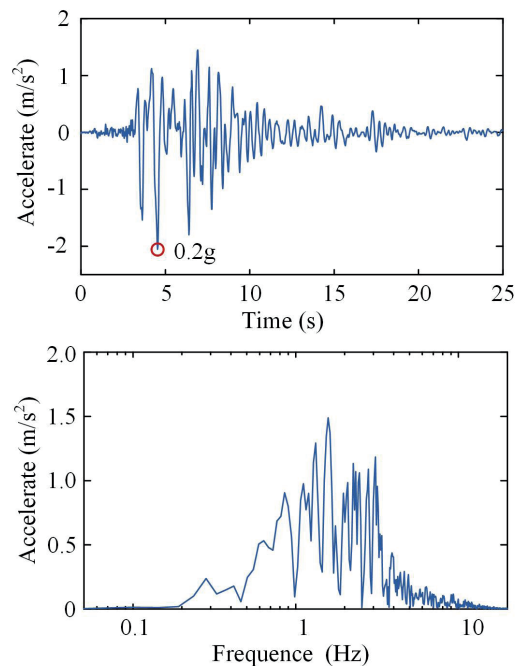


Fig. 4 The curves of the seismic wave time-histories and the Fourier spectrum

residual pore water pressure around the pile foundation caused by dynamic load, so a simplified and conserved application method of load is selected [6, 24, 38]. In addition, a monopile and hybridpile of 30 m and 20 m are used. Considering that the steel bar consumption of different pile types is similar economically, so their work conditions calculated by numerical simulation are shown in Table 3.

3.2 Numerical simulation of load application

In order to exclude the influence of boundary effect on numerical calculation results and shorten the model calculation time as possible, the calculation area of the soil surrounding pile foundation should be appropriately considered before modeling. For the soil calculation domain, a length of 60 m is taken in X direction, a length of 40 m is taken in Y direction, and a length of 60 m is taken in Z direction. At the same time, some local grids of the soil surrounding pile foundation are divided more finely to improve calculation accuracy. The model of hybridpile contains 51797 nodes and 47770 elements, and the model of monopile contains 33403 nodes and 30347 elements. In addition, for the constitutive models of shear-volumetric strain coupled incremental pore pressure soil, it is needed to get the initial effective confining pressure of the soil under gravity stress, therefore, before performing explicit dynamic analysis, it is necessary to utilize static analysis steps to apply gravity to the entire model for calculating the initial effective confining pressure of the soil. Meanwhile, a crustal stress equilibrium analysis should be carried out to eliminate the deformations caused by model's gravity stress.

For the working condition that only wind and wave loading are considered, through exerting a time-varying pressure on seabed surface, we can simulate the dynamic effect of water pressure changes caused by wave rise and fall on the seabed soil [39]. Then, the time histories of pore water pressure in the pile foundation's surrounding soil region

and in seabed soil region are extracted from the numerical results, and the impact of the presence of pile foundation on the growth of seabed pore water pressure is compared. The water pressure change is simplified as harmonic pressure load, the load frequency is set as 0.25 Hz, the pressure amplitude is set as 50 kPa, and the above-seabed standing level elevation is 10 m. The time-varying water pressure can be realized by calling the VLOAD subroutine of ABAQUS/Explicit that has been compiled. The wind and wave load on the pile foundation is simplified as concentrated node force, which is applied on the top of the tower and the top of the pile foundation, respectively. The wind load on the tower is simplified as static load, while the wave load on the pile foundation is simplified as harmonic load.

For the working conditions considering earthquake load, due to the gravity stress applied on the model, so the lateral boundary of the soil calculation domain cannot adopt free boundary or fixed boundary according to traditional boundary setting method [31, 40], but using a removable flexible boundary constrained by nodal forces. In this way, the lateral displacement caused by model gravity can be effectively constrained, while ensuring that the model can be compatibly deformed under seismic action. Since the lateral boundary of the soil model is fixed constrained when the ground stress is balanced, the node reaction force (RF) can be calculated by the lateral boundary constraints force caused by the heavy stress through the result of the static analysis. The derived RF value is input to the node of the model's lateral boundary through compiling the Python script to achieve flexible boundary constraints. The schematic diagram of above load application method and boundary conditions is shown in Fig. 5.

Table 3 Working condition calculated by numerical simulation

Case	Pile type	Pile length	Loading method
1	Hybridpile	20 m	Wind & wave loading
2	Hybridpile	20 m	Seismic loading
3	Hybridpile	20 m	Wind & wave loading and Seismic loading
4	Monopile	30 m	Wind & wave loading
5	Monopile	30 m	Seismic loading
6	Monopile	30 m	Wind & wave loading and Seismic loading

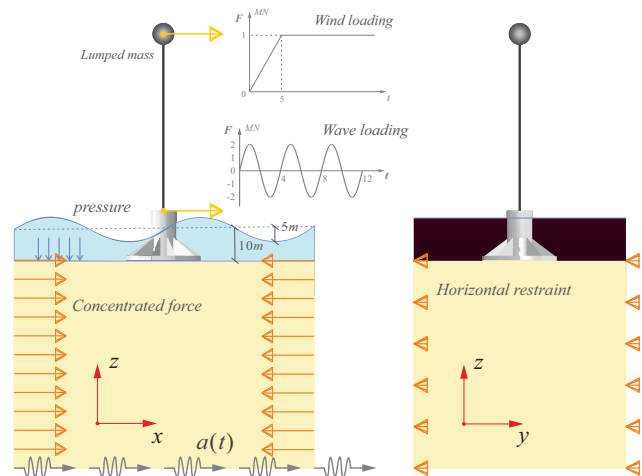


Fig. 5 Schematic diagram of loading applying method and boundary conditions

4 Response to dynamic loading

By using the calculation results of numerical model and taking a monopile model as a reference model, the influence of environmental loading on hybrid foundation's loading performance as well as the changes in residual pore water pressure around the pile foundation caused by dynamic loads are compared. Since the actual value of the pore water pressure cannot reflect the liquefy action degree of the soil region, so the pore water pressure ratio r_u mentioned in the second chapter is used to reflect the pore water pressure distribution and variation of the soil region.

Fig. 6 shows the distribution of pore water pressure ratio r_u along the monopile and hybridpile obtained from vertical sections of pile foundation along centerline. It can be seen that the areas where pore water pressure accelerates to accumulate under different working conditions are all located at the cylinder flange, rather than the contact surface of pile foundation and soil. In addition, for the hybrid foundation, the pore water pressure accumulated caused by seismic loading is higher than that due to wind and wave loading. This is because the integral stiffness of hybrid foundation is greater than the soil, so the hybrid foundation

is not easily deformable as the soil under an earthquake, and a greater contact force can generate under soil-structure interaction, leading to a faster accumulation of pore pressure. The residual pore water pressure accumulation of monopile foundation's surrounding soil is not obvious under earthquake, and the pore water pressure accumulation area is obviously around the monopile foundation under a joint action of wind, wave and seismic loading.

In order to analyze the effect of pile foundation on the pore water pressure accumulation of seabed soil, the residual pore water pressure ratio r_u time-histories of four observation points A, B, C and D is selected. These four observation points are arranged data fixed distance of 5 m, and the detection point is 1m below the seabed surface. For a hybrid foundation, the observation points A and B are respectively positioned at monopile and cylinder flange, see schematic diagrams in Fig. 7.

According to Fig. 8, the pore water pressure ratio r_u time-histories of monopile and the hybridpile at observation point A are compared, and the monopile's r_u values at point A under different working conditions are all higher than hybrid foundation, which is because the cylindrical platform

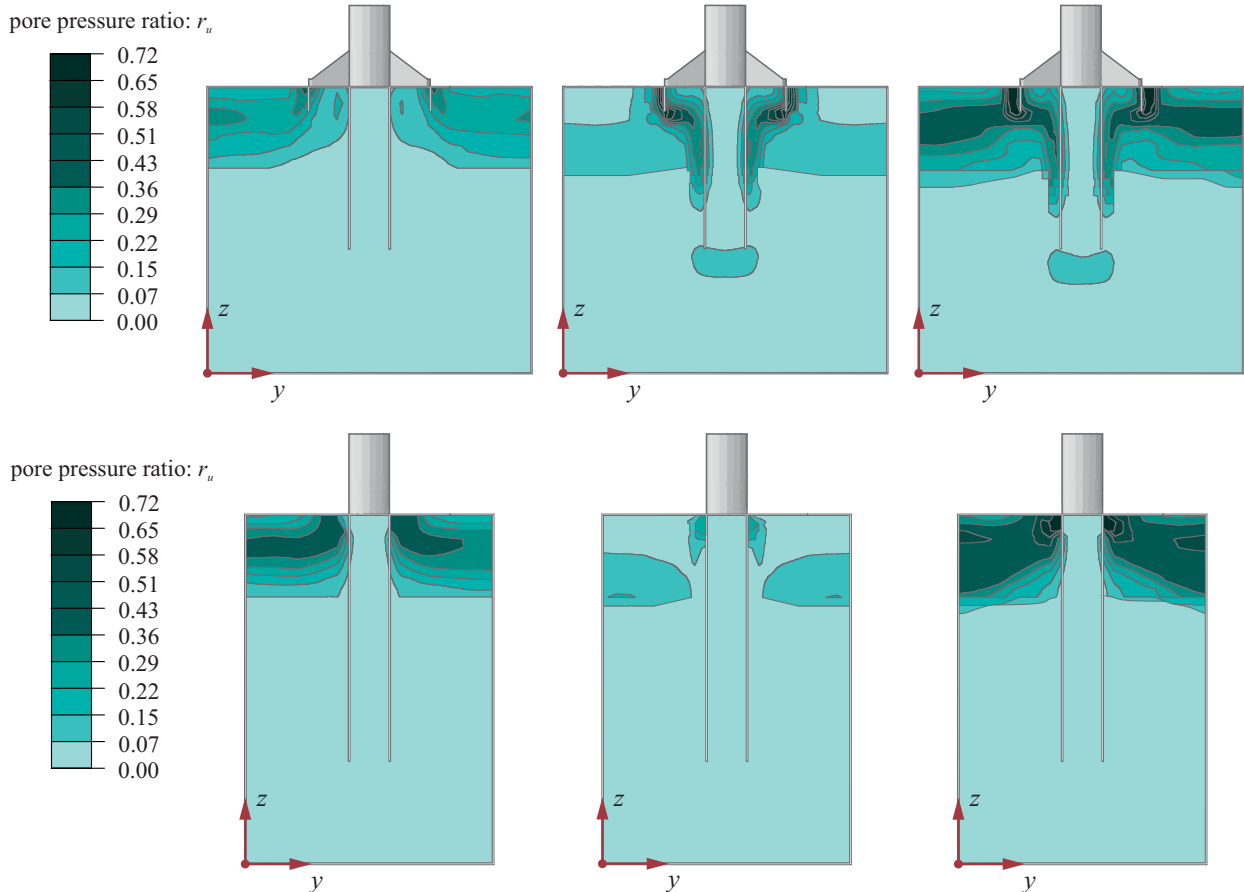


Fig. 6 Distribution diagram of residual pore pressure ratio r_u around pile

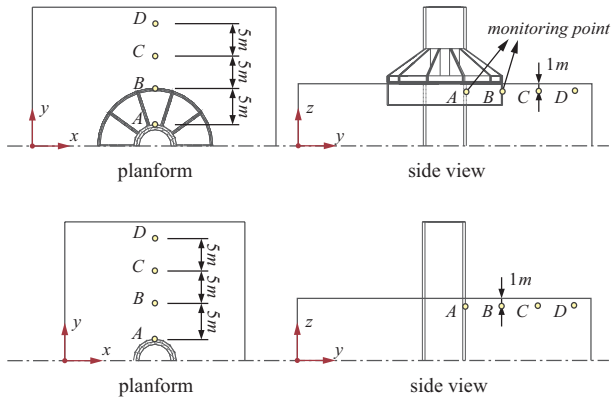


Fig. 7 Schematic diagram of extraction position of residual pore pressure ratio

of hybrid foundation limits the interaction between middle piles and the soil to some extent. The situations of the detection points B and C are just opposite: the hybrid foundation's r_u value at observation point B are all higher than monopile foundation, but compared to point B, the r_u value gap of two pile foundations at point C is reduced. At point D, the two pile type's r_u values are very close, indicating that

the impact of the existence and type of pile foundation on the seabed soil's pore water pressure accumulation in this region has been gradually weakened. Besides, it can be discovered from the four graphs in the middle that the residual pore water pressure of soil surrounding the hybrid foundation is much higher than the monopile foundation caused by seismic loading, which coincides with the conclusion that the pore pressure accumulation of hybrid foundation caused by earthquake is higher as shown in Fig. 6. From the right-most four sub-graphs, the seismic action will further accelerate the accumulation of pore water pressure, especially for the hybrid foundation.

Fig. 9 shows the horizontal distribution of pore water pressure ratio r_u of the seabed surface around the pile foundation. From Fig. 9, the presence of the hybrid foundation's cylindrical platform changes the residual pore water pressure accumulation region under environmental loads. For monopile foundation, the pore pressure is more easily to accumulate at the contact position between monopile surface and soil under dynamic loading. For hybrid

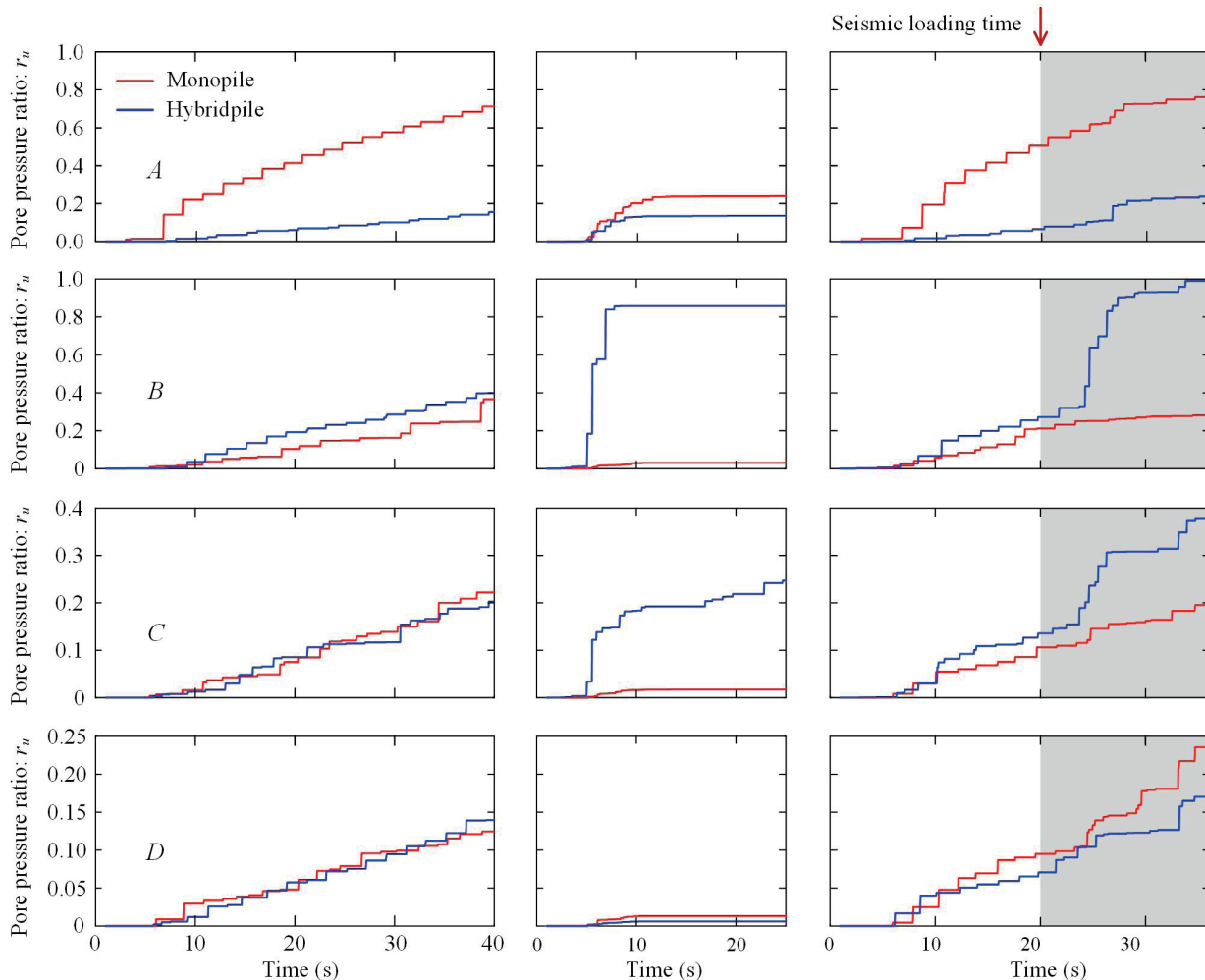


Fig. 8 Time history of residual pore pressure ratio at different monitors

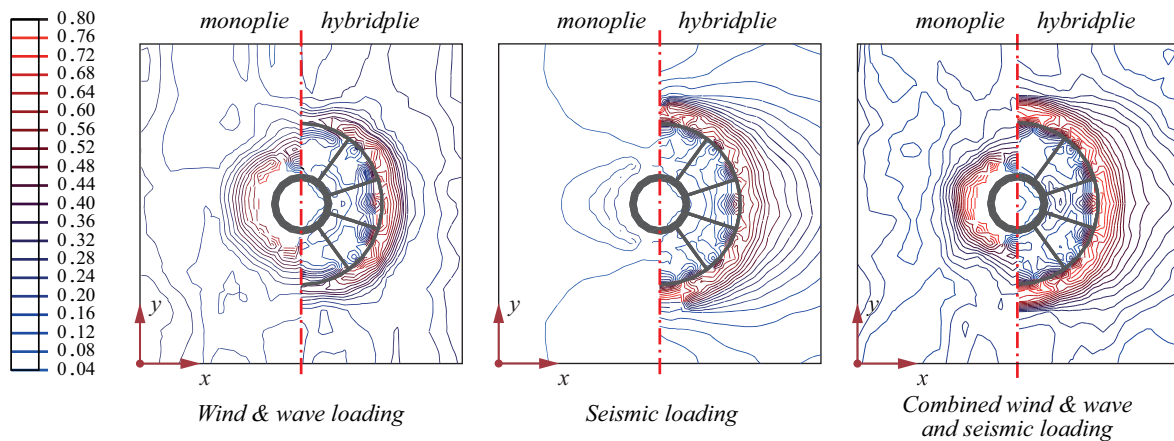


Fig. 9 Comparison of pore pressure ratio ru between monopile and hybridpile on the seabed surface

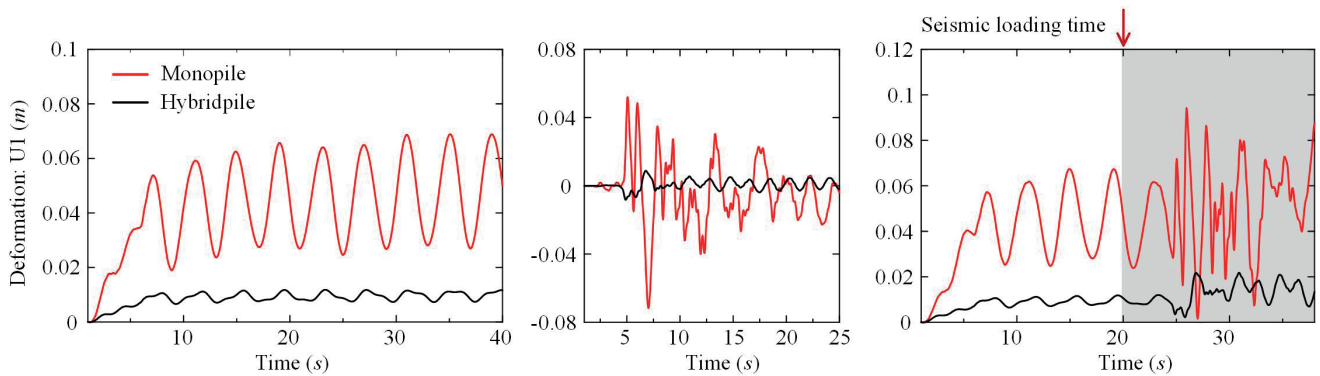


Fig. 10 Displacement envelope along pile depth between monopile and hybridpile

foundation, soil liquefaction is more likely to happen at the contact position between cylindrical platform and soil, and then pore pressure accelerates accumulation area to transfer. In addition, the middle graph of Fig. 9 further concludes that the monopile foundation is only less likely to cause soil pore pressure accumulation under earthquake.

In order to further study the horizontal deformation resistance performance of hybrid foundation with pile length of 30 m, a monopile foundation with pile length of 30 m is served as a control group, and the pile top displacement time-histories of two pile types under different working conditions are extracted, as shown in Fig. 10. The left diagram represents the pile top displacement time-histories of two pile types under wind and wave loading, the middle diagram represents the pile top displacement time-histories under seismic loading, and the right diagram represents the pile top displacement time-histories under a joint action of wind, wave and seismic loading. In Fig. 10, it's obvious that although the pile length of hybrid foundation is shorter than monopile foundation, the pile top displacement time-histories of hybrid foundation under different conditions are all less than the monopile

foundation due to the presence of the cylindrical platform. This shows that the cylindrical platform can significantly reduce the horizontal displacement of pile top.

5 Conclusions

This paper studies the dynamic response characteristics of innovative OWTs's hybrid foundation under wind, wave and seismic loading, and uses the incremental pore pressure constitutive model to simulate the kinetic behavior of soil. Considering the distribution characteristics and time-history change of residual pore water pressure surrounding pile foundation caused by tower-pile foundation-saturated soil interactions, it is concluded as below:

(1) By comparing the pore water pressure ratio distribution and time-histories surrounding monopile and hybrid foundation under different loads, it can be derived that the hybrid foundation's cylindrical platform changes the residual pore water pressure accumulation area. For monopile foundation, the residual pore water pressure accumulation area is mainly surrounding the pile foundation, but the pore water pressure accumulation area is mainly near the cylindrical platform for hybrid foundation.

(2) If only considering the working condition under the seismic loading, compared to hybrid foundation, the peak of residual pore water pressure accumulated surrounding monopile foundation is smaller, which is due to the lower basic structural stiffness of monopile foundation. Thus, considering the pile foundation-soil interaction, the monopile foundation is easier to deform with the soil.

(3) In case that a cylindrical platform structure is added, although shorter monopile foundations are used as their middle piles, the horizontal displacement extreme of hybrid foundation is still smaller than that of longer monopile foundation under environmental loading, demonstrating a superior horizontal deformation resistance of new hybrid foundation than monopile foundation.

References

- [1] Anastasopoulos, I., Theofilou, M. "Hybrid foundation for offshore wind turbines: Environmental and seismic loading", *Soil Dynamics and Earthquake Engineering*, 80, pp. 192–209, 2016.
<https://doi.org/10.1016/j.soildyn.2015.10.015>
- [2] Wang, P., Zhao, M., Du, X., Liu, J., Xu, C. "Wind, wave and earthquake responses of offshore wind turbine on monopile foundation in clay", *Soil Dynamics and Earthquake Engineering*, 113, pp. 47–57, 2018.
<https://doi.org/10.1016/j.soildyn.2018.04.028>
- [3] Chen, D., Huang, K., Bretel, V., Hou, L. "Comparison of structural properties between monopile and tripod offshore wind-turbine support structures", *Advances in Mechanical Engineering*, 5, 175684, 2013.
<https://doi.org/10.1155/2013/175684>
- [4] Chen, D., Gao, P., Huang, S., Fan, K., Zhuang, N., Liao, Y. "Dynamic response and mooring optimization of spar-type substructure under combined action of wind, wave, and current", *Journal of Renewable and Sustainable Energy*, 9(6), 063307, 2017.
<https://doi.org/10.1063/1.5017228>
- [5] Page, A. M., Grimstad, G., Eiksund, G. R., Jostad, H. P. "A macro-element pile foundation model for integrated analyses of monopile-based offshore wind turbines", *Ocean Engineering*, 167, pp. 23–35, 2018.
<https://doi.org/10.1016/j.oceaneng.2018.08.019>
- [6] Kourkoulis, R. S., Lekakakis, P. C., Gelagoti, F. M., Kaynia, A. M. "Suction caisson foundations for offshore wind turbines subjected to wave and earthquake loading: effect of soil–foundation interface", *Géotechnique*, 64(3), pp. 171–185, 2014.
<https://doi.org/10.1680/geot.12.P.179>
- [7] Leblanc, C., Houlsby, G. T., Byrne, B. W. "Response of stiff piles in sand to long-term cyclic lateral loading", *Géotechnique*, 60(2), pp. 79–90, 2010.
<https://doi.org/10.1680/geot.7.00196>
- [8] Rad, M. M. "Reliability Based Analysis and Optimum Design of Laterally Loaded Piles", *Periodica Polytechnica Civil Engineering*, 61(3), pp. 491–497, 2017.
<https://doi.org/10.3311/PPci.8756>
- [9] Rad, M. M., Ibrahim, S. K. "Optimal Plastic Analysis and Design of Pile Foundations Under Reliable Conditions", *Periodica Polytechnica Civil Engineering*, 65(3), pp. 761–767, 2021.
<https://doi.org/10.3311/PPci.17402>
- [10] Rad, M. M., Ibrahim, S. K., Lógó, J. "Limit design of reinforced concrete haunched beams by the control of the residual plastic deformation", *Structures*, 39, pp. 987–996, 2022.
<https://doi.org/10.3311/PPci.8756>
- [11] Seed, H. B., Rahman, M. S. "Wave-induced pore pressure in relation to ocean floor stability of cohesionless soils", *Marine Georesources and Geotechnology*, 3(2), pp. 123–150, 1978.
<https://doi.org/10.1080/10641197809379798>
- [12] Jeng, D.-S., Zhao, H. Y. "Two-dimensional model for accumulation of pore pressure in marine sediments", *Journal of Waterway, Port, Coastal, and Ocean Engineering*, 141(3), 04014042, 2015.
[https://doi.org/10.1061/\(ASCE\)WW.1943-5460.0000282](https://doi.org/10.1061/(ASCE)WW.1943-5460.0000282)
- [13] Zhao, H. Y., Jeng, D.-S., Liao, C. C., Zhu, J. F. "Three-dimensional modeling of wave-induced residual seabed response around a mono-pile foundation", *Coastal Engineering*, 128, pp. 1–21, 2017.
<https://doi.org/10.1016/j.coastaleng.2017.07.002>
- [14] Zhu, B., Ren, J., Ye, G.-L. "Wave-induced liquefaction of the seabed around a single pile considering pile–soil interaction", *Marine Georesources and Geotechnology*, 36(1), pp. 150–162, 2018.
<https://doi.org/10.1080/1064119X.2017.1340374>
- [15] Sui, T., Zhang, C., Jeng, D., Guo, Y., Zheng, J., Zhang, W., Shi, J. "Wave-induced seabed residual response and liquefaction around a mono-pile foundation with various embedded depth", *Ocean Engineering*, 173, pp. 157–173, 2019.
<https://doi.org/10.1016/j.oceaneng.2018.12.055>
- [16] Liao, C., Chen, J., Zhang, Y. "Accumulation of pore water pressure in a homogeneous sandy seabed around a rocking mono-pile subjected to wave loads", *Ocean Engineering*, 173, pp. 810–822, 2019.
<https://doi.org/10.1016/j.oceaneng.2018.12.072>
- [17] Kjørlaug, R. A., Kaynia, A. M. "Vertical earthquake response of megawatt-sized wind turbine with soil-structure interaction effects", *Earthquake Engineering & Structural Dynamics*, 44(13), pp. 2341–2358, 2015.
<https://doi.org/10.1002/eqe.2590>

In brief, the existence of the cylindrical platform can change the distribution of the residual pore water pressure surrounding the pile and delay liquefaction around the pile, and it can significantly reduce the horizontal displacement and bending moment extreme of pile foundation under the environment loads. Therefore, the novel hybrid pile foundation is worth considering and promoting in the design of offshore pile foundation.

Acknowledgement

The project presented in this article is supported by National Key Research and Development Program (2017YFC1500804) and Hubei Natural Science Foundation (2021CFA035).

- [18] De Risi, R., Bhattacharya, S., Goda, K. "Seismic performance assessment of monopile-supported offshore wind turbines using unscaled natural earthquake records", *Soil Dynamics and Earthquake Engineering*, 109, pp. 154–172, 2018.
<https://doi.org/10.1016/j.soildyn.2018.03.015>
- [19] Bienen, B., Dührkop, J., Grabe, J., Randolph, M. F., White, D. J. "Response of piles with wings to monotonic and cyclic lateral loading in sand", *Journal of Geotechnical and Geoenvironmental Engineering*, 138(3), pp. 364–375, 2012.
[https://doi.org/10.1061/\(ASCE\)GT.1943-5606.0000592](https://doi.org/10.1061/(ASCE)GT.1943-5606.0000592)
- [20] Wang, X., Zeng, X., Yang, X., Li, J. "Feasibility study of offshore wind turbines with hybrid monopile foundation based on centrifuge modeling", *Applied Energy*, 209, pp. 127–139, 2018.
<https://doi.org/10.1016/j.apenergy.2017.10.107>
- [21] Wang, X., Zeng, X., Li, X., Li, J. "Investigation on offshore wind turbine with an innovative hybrid monopile foundation: An experimental based study", *Renewable Energy*, 132, 129–141, 2019.
<https://doi.org/10.1016/j.renene.2018.07.127>
- [22] Wang, X., Zeng, X., Li, X., Li, J. "Liquefaction characteristics of offshore wind turbine with hybrid monopile foundation via centrifuge modelling", *Renewable Energy*, 145, pp. 2358–2372, 2020.
<https://doi.org/10.1016/j.renene.2019.07.106>
- [23] Chen, G., Zhao, D., Chen, W., Juang, C. H. "Excess pore-water pressure generation in cyclic undrained testing", *Journal of Geotechnical and Geoenvironmental Engineering*, 145(7), 04019022, 2019.
[https://doi.org/10.1061/\(ASCE\)GT.1943-5606.0002057](https://doi.org/10.1061/(ASCE)GT.1943-5606.0002057)
- [24] Chen, D., Gao, P., Huang, S., Li, C., Yu, X. "Static and dynamic loading behavior of a hybrid foundation for offshore wind turbines", *Marine Structures*, 71, 102727, 2020.
<https://doi.org/10.1016/j.marstruc.2020.102727>
- [25] Damgaard, M., Zania, V., Andersen, L. V., Ibsen, L. B. "Effects of soil-structure interaction on real time dynamic response of offshore wind turbines on monopiles", *Engineering Structures*, 75, pp. 388–401, 2014.
<https://doi.org/10.1016/j.engstruct.2014.06.006>
- [26] Damgaard, M., Bayat, M., Andersen, L. V., Ibsen, L. B. "Assessment of the dynamic behaviour of saturated soil subjected to cyclic loading from offshore monopile wind turbine foundations", *Computers and Geotechnics*, 61, pp. 116–126, 2014.
<https://doi.org/10.1016/j.compgeo.2014.05.008>
- [27] Wang, X., Zeng, X., Yang, X., Li, J. "Seismic response of offshore wind turbine with hybrid monopile foundation based on centrifuge modelling", *Applied Energy*, 235, pp. 1335–1350, 2019.
<https://doi.org/10.1016/j.apenergy.2018.11.057>
- [28] Deb, T. K., Singh, B. "Response and capacity of monopod caisson foundation under eccentric lateral loads", *Marine Georesources & Geotechnology*, 36(4), pp. 452–464, 2018.
<https://doi.org/10.1080/1064119X.2017.1330374>
- [29] Long, H., Wang, Z., Zhang, C., Zhuang, H., Chen, W., Peng, C. "Nonlinear study on the structure-soil-structure interaction of seismic response among high-rise buildings", *Engineering Structures*, 242, 112550, 2021.
<https://doi.org/10.1016/j.engstruct.2021.112550>
- [30] Ruan, B., Ji, H., Ye, Y., Wang, S., He, H., Li, J., Miao, Y. "A numerical separation method for incident wave of ground motion in time domain", *Soil Dynamics and Earthquake Engineering*, 163, 107550, 2022.
<https://doi.org/10.1016/j.soildyn.2022.107550>
- [31] Chen, G., Ruan, B., Zhao, K., Chen, W., Zhuang, H., Du, X., Khoshnevisan, S., Juang, C. H. "Nonlinear response characteristics of undersea shield tunnel subjected to strong earthquake motions", *Journal of Earthquake Engineering*, 24(3), pp. 351–380, 2020.
<https://doi.org/10.1080/13632469.2018.1453416>
- [32] Ruan, B., Zhao, K., Wang, S.-Y., Chen, G.-X., Wang, H.-Y. "Numerical Modeling of Seismic Site Effects in a Shallow Estuarine Bay (Suai Bay, Shantou, China)", *Engineering Geology*, 260, 105233, 2019.
<https://doi.org/10.1016/j.enggeo.2019.105233>
- [33] Zhao, K., Wang, Q., Zhuang, H., Li, Z., Chen, G. "A fully coupled flow deformation model for seismic site response analyses of liquefiable marine sediments", *Ocean Engineering*, 251, 111144, 2022.
<https://doi.org/10.1016/j.oceaneng.2022.111144>
- [34] Martin, G. R., Seed, H. B., Finn, W. D. L. "Fundamentals of liquefaction under cyclic loading", *Journal of the Geotechnical Engineering Division*, 101(5), pp. 423–438, 1975.
<https://doi.org/10.1061/AJGEB6.0000164>
- [35] Chen, G., Wang, Y., Zhao, D., Zhao, K., Yang, J. "A new effective stress method for nonlinear site response analyses", *Earthquake Engineering & Structural Dynamics*, 50(6), pp. 1595–1611, 2021.
<https://doi.org/10.1002/eqe.3414>
- [36] Dobry, R., Ladd, R. S., Yokel, F. Y., Chung, R. M., Powell, D. "Prediction of Pore Water Pressure Buildup and Liquefaction of Sands during Earthquakes by the Cyclic Strain Method", US Department of Commerce, National Bureau of Standards, Washington, DC, USA, 1982.
- [37] Lombardi, D., Bhattacharya, S., Wood, D. M. "Dynamic soil-structure interaction of monopile supported wind turbines in cohesive soil", *Soil Dynamics and Earthquake Engineering*, 49, pp. 165–180, 2013.
<https://doi.org/10.1016/j.soildyn.2013.01.015>
- [38] Jin, L., Zhu, J., Zhou, W., Liang, J., Chen, G. "2D dynamic tunnel-soil-aboveground building interaction I: Analytical solution for incident plane SH-waves based on rigid tunnel and foundation model", *Tunnelling and Underground Space Technology*, 128, 104625, 2022.
<https://doi.org/10.1016/j.tust.2022.104625>
- [39] Zhao, H.-Y., Jeng, D.-S. "Numerical study of wave-induced soil response in a sloping seabed in the vicinity of a breakwater", *Applied Ocean Research*, 51, pp. 204–221, 2015.
<https://doi.org/10.1016/j.apor.2015.04.008>
- [40] Xu, C., Song, J., Du, X., Zhao, M. "A local artificial-boundary condition for simulating transient wave radiation in fluid-saturated porous media of infinite domains", *International Journal for Numerical Methods in Engineering*, 112(6), pp. 529–552, 2017.
<https://doi.org/10.1002/nme.5525>